Developmental loss of miniature *N*-methyl-D-aspartate receptor currents in NR2A knockout mice

Matthew Townsend*, Akira Yoshii†, M. Mishina‡, and Martha Constantine-Paton§¶

*Interdepartmental Neuroscience Program, Yale University, New Haven, CT 06520; †Department of Neurology, Massachusetts General Hospital, Boston, MA 02114; ‡Department of Molecular Neurobiology and Pharmacology, University of Tokyo School of Medicine, 7-3-1 Hongo, Bunkyo-ku, Tokyo 113-0033, Japan; and §Departments of Biology and Brain and Cognitive Science and the McGovern Institute for Brain Research, Massachusetts Institute of Technology, Cambridge, MA 02139

Edited by Charles F. Stevens, The Salk Institute for Biological Studies, La Jolla, CA, and approved December 9, 2002 (received for review September 24, 2002)

The *N*-methyl-D-aspartate (NMDA) glutamate receptor (NMDAR), long implicated in developmental plasticity, shows decay time kinetics that shorten postnatally as NR2A subunits are added to the receptor. Neither the mechanism nor immediate effect of this change is known. We studied developing NMDAR currents by using visual neurons in slices from NR2A knockout (NR2AKO) and WT mice. Both strains show increased dendritic levels of synaptic density scaffolding protein PSD-95 with age. Dendritic levels of NR2A increased at the same time in WT and immunoprecipitated with PSD-95. PSD-95/NMDAR binding was significantly decreased in the NR2AKO. Moreover, NMDAR miniature currents (minis) were lost and rise times of NMDAR evoked currents increased in mutant mice. Age-matched WT cells showed NR2A-rich receptors predominating in minis, yet slow NR2B mediated currents persisted in evoked currents. Disrupting photoreceptor activation of retinal ganglion cells eliminated increases in PSD-95 and NR2A in superior collicular dendrites of WT mice and slowed the loss of miniature NMDAR currents in NR2AKOs. These data demonstrate that NMDARs that respond to single quantal events mature faster during development by expressing the NR2A subunit earlier than NMDARs that respond to evoked release. We hypothesize that NR2A-rich NMDARs may be localized to the center of developing synapses by an activity-dependent process that involves the targeting of PSD-95 to the postsynaptic density. Neonatal receptors become restricted to perisynpatic or extrasynaptic sites, where they participate primarily in evoked currents.

In visual pathways, *N*-methyl-D-aspartate (NMDA) receptors (NMDARs) contain NR1 (GluR ζ1) plus varying proportions of NR2A (GluR ε1) and NR2B (GluR ε2) subunits (1, 2). The decay times of evoked NMDAR currents (NMDARcs) become faster during development as NR2A is incorporated (3–6). Reducing visual activity, delays synaptic refinement in the visual cortex (VC) (7, 8), delays the shortening of NMDRc decay time (9) and up-regulation of NR2A (10). Furthermore dark-reared rats rapidly up-regulate NR2A at cortical synapses upon light exposure, whereas rats placed in darkness down-regulate NR2A in dendrites over several days (11, 12). The mechanism of this rapid activity-dependent trafficking is unknown, but related work in our laboratory suggests that scaffolding of the NMDAR by PSD-95 may be involved.

Methods

Animals. All surgical procedures were compliant with the Massachusetts Institute of Technology Committee on Animal Care (CAC) animal protocol review. WT C57BL/6 mice and NR2AKO mice (13) with a C57BL/6 background were used in all experiments. All animals were killed before eye opening on postnatal day 13 (P13).

Surgery. Preparation of Elvax plastic (DuPont) for drug delivery in the eye was carried out as in ref. 14. Glutamate antagonists were dissolved in DMSO and Elvax [MK801 final concentration = 6 mM, estimated active concentration in eye = 200 μM and 2,3-dihydroxy-6-nitro-7-sulfamoylbenzo[*f*]quinoxaline (NBQX) final concentration = 600 μM, estimated active concentration in eye = 20 μM]. Control Elvax contained solvent alone. Slivers of Elvax were inserted behind the lens through a small incision at the ciliary margin on P6. Eyelids were reshut with sutures and Vetbond, but opened before death to access the effectiveness of the light evoked response by using a penlight and the pupilary reflex. Blockade was restricted to glutamate receptors in the eyecup, because only the sSC contralateral to the eye containing α-amino-3-hydroxy-5-methyl-4-isoxazole propionic acid receptor (AMPAR) and NMDAR antagonists failed to up-regulate PSD-95 and NR2A (Fig. 5*D*).

Western Blotting. Synaptoneurosomes (crude neuropil fractions) were prepared from the superficial layers of the superior colliculus (sSC) of P8–P11 mice according to published methods (15–17).

Immunoprecipitations were performed by using deoxycholate soluble membrane fractions (18). Blots from SDS/6–8% PAGE gels were probed with antibodies to NR1 (PharMingen), NR2A, NR2B (Molecular Probes, Transduction Labs, Chemicon), Actin (Sigma), and PSD-95 (Upstate Biotechnology) and reacted for chemiluminesence (Pierce). Film exposures were in the linear range for all bands being compared. Band density was quantified as described by using NIH IMAGE and its gel-plotting macros (2). At least three separate protein isolations were made at all time points and averaged for quantitation.

Electrophysiology. Pups anesthetized with isoflurane were decapitated, and the midbrain was dissected. Recordings were from neurons of the stratum griseum superficiale of 350-μm parasagital collicular slices. Slices equilibrated in 117 mM NaCl/3 mM $MgCl_2$/4 mM KCl/3 mM $CaCl_2$/1.2 mM $NaHPO_4$/26 mM $NaHCO_3$/16 mM glucose for at least 1 h before recording. Glass pipettes were filled with 122.5 mM Cs-gluconate/17.5 mM CsCl/10 mM Hepes (CsOH)/0.2 mM Na-EGTA/2 mM Mg-ATP/0.3 mM Na-GTP/8 mM NaCl with 0.2% biocytin at pH 7.3. Cells had resting potentials of ≈ -50 mV and were voltage-clamped at either + 40 or -70 mV. NMDARcs were isolated by the addition of antagonists for γ-aminobutyric acid (GABA) type A receptors (bicuculline, 10 μM) and AMPA/kainate receptors (GYKI 52466 or 6,7-dinitroquinoxaline-2,3-dione, 10 μM). At -70 mV the recording medium contained 0 mM Mg^{2+}. Neurons maintained seal resistances between 1 and 3 GΩ. Access resistance was <40 MΩ. Pipette and whole cell capacitance was compensated.

For each neuron studied average spontaneous NMDARcs were from events collected over a 2- to 4-min period after a solution exchange period (5 min). Spontaneous events were

This paper was submitted directly (Track II) to the PNAS office.

Abbreviations: NMDA, *N*-methyl-D-aspartate; NMDAR, NMDA receptor; NMDARc, NMDAR current; sSC, superficial layers of the superior colliculus; AMPAR, α-amino-3-hydroxy-5-methyl-4-isoxazole propionic acid receptor; GABA, γ-aminobutyric acid; P*n*, postnatal day *n*.

¶To whom correspondence should be addressed. E-mail: mcpaton@mit.edu.

www.pnas.org/cgi/doi/10.1073/pnas.0335786100

considered synaptic if they had rise times <8–9 ms and peak amplitudes at least two times baseline to peak noise (1.5 pA). Spontaneous events (15–30) were averaged by using MINIANALYSIS software (SynaptoSoft). When AMPA as well as $GABA_A$ receptors were blocked, the frequency of spontaneous NMDARcs dropped significantly. Further addition of tetrodotoxin to block action potentials reduced NMDARc frequency by <5% indicating that nearly all of these events were miniature NMDARcs.

Electrical stimuli consisted of 5–70 μAMP, 0.2-ms pulses delivered to the stratum opticum at 0.2 Hz through paired tungsten or platinum–iridium electrodes (tip separation ≈50 microns). In low-Ca^{2+}/high-Mg^{2+} experiments, Ca^{2+} concentration was adjusted to 15 μM: the concentration where spontaneous miniature currents (minis) in WT mice were frequent enough to permit analyses but still fell in the same size range as "evoked" minis in 0 mM Ca^{2+}.

The "evoked mini frequency adj" histogram in Fig. 4*E* was calculated by comparing the number of evoked miniature NMDARcs that occurred before and after ifenprodil for each cell. Differences in mini frequency were treated as though events that fell below the level of detectability, and were conservatively assumed to have an amplitude of 0 pA. The percent ifenprodil block was recalculated by this adjustment, and was significantly different from evoked NMDARcs in the same cells (see Fig. 7, which is published as supporting information on the PNAS web site, www.pnas.org).

Results

Selective Loss of Spontaneous NMDARcs in NR2AKOs. Spontaneous NMDARcs were studied in midbrain slices from NR2AKO and WT mice with AMPA and $GABA_A$ receptors blocked. Under these conditions ≈95% of spontaneous NMDARcs are miniature events (spon/minis), see *Methods*. In WT mice, spontaneous excitatory postsynaptic potentials and spon/mini NMDARc amplitudes remained constant between P8 and P13 (Fig. 1 *A* and *B*) (2). In this interval spon/mini NMDARcs in the NR2AKO showed a progressive decay in amplitude terminating at ~P13, when NMDARcs were indistinguishable from baseline noise (<3 pA at −70 mV; Fig. 1 *C* and *D*). Application of the glutamate transporter antagonist TBOA to P11 neurons in NR2AKO mice partially restored spon/mini NMDARcs (Fig. 1*D*). Thus spon/mini NMDARcs are lost between P8 and P13 in NR2AKOs, but recover significantly when glutamate diffusion is prolonged.

In contrast to spon/mini currents, evoked NMDARcs persisted in mutant mice with decay times that did not differ significantly from WT (Fig. 2*A*). However, rise times of evoked NMDARcs in NR2AKOs were significantly slower by P13 compared with either WT or P8 mutant mice (Fig. 2*B*). In addition, the NMDARc/AMPAR currents (AMPARcs) amplitude ratio was significantly reduced in the NR2AKO by P13 (Fig. 8, which is published as supporting information on the PNAS web site). (Spontaneous AMPARcs amplitudes remained constant between P8 and P13 in both WT and NR2AKO mice). Similar changes have been reported in mice with a C-terminal truncation of NR2A, where the data suggest that the inability to anchor NMDARs causes a loss of receptor density immediately beneath glutamate release sites (19).

Spontaneous and evoked AMPARcs were examined in WT and NR2AKO animals to determine whether the absence of NR2A affected presynaptic cleft dimensions or transmitter release. No significant differences were observed between P8 and P13 knockout and WT neurons in evoked AMPARc rise times or in spontaneous AMPARc amplitude or (Fig. 8). Paired pulse ratios (20- and 40-ms interpulse interval) also did not differ between NR2AKO and WT (n = 7 WT, 5 NR2AKO P12–P13 neurons), suggesting that transmitter release was not altered in the mutant animals (Fig. 9, which is published as supporting information on the PNAS web site).

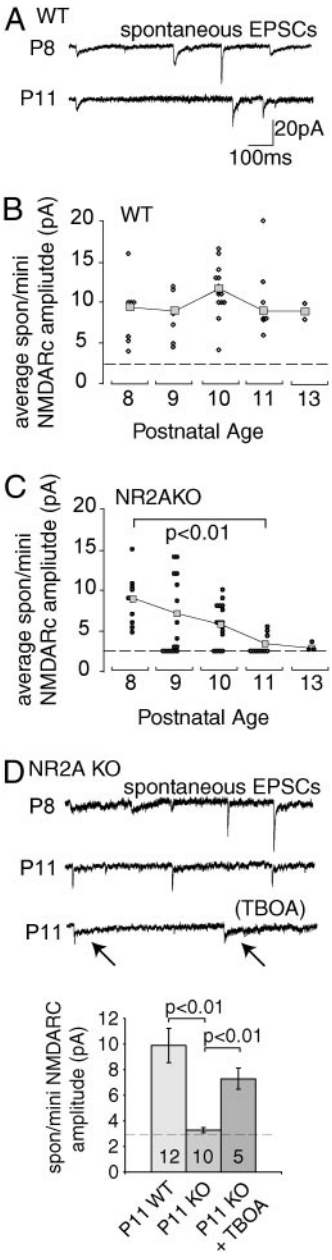

Fig. 1. Spontaneous and mini NMDARcs disappear in NR2AKO mice. Excitatory field potential currents were recorded at −70 mV in 0 mM Mg^{2+} with $GABA_A$ receptors blocked. With both AMPA and $GABA_A$ receptors blocked, 95% of spontaneous NMDARcs are miniature events and are labeled as spon/mini NMDARcs. (*A*) AMPARcs/NMDARcs recorded in P8 and P11 WT neurons. (*B*) WT, average spon/mini NMDARc amplitudes (squares) were not significantly different between P8 and P13 (ANOVA Tukey–Kramer post hoc, $P = 0.24$). Circles represent average spon/mini NMDARc amplitudes for individual neurons. Dotted lines represent threshold for detectablity. (*C*) Spon/mini NMDARc current amplitudes fall to noise levels by P13 in NR2AKO mice (ANOVA Tukey–Kramer post hoc P8 and P13). (*D*) AMPARcs/NMDARcs recorded in P8 and P11 NR2AKO neurons. The NMDARc component is gone on P11 in this cell, whereas AMPARcs persist. NMDARcs reappeared in the recording (arrows), when perfusion contained TBOA. Tabulated amplitude decreases between spon/mini NMDARcs in NR2AKO, and WT P11 neurons partially disappear in the presence of TBOA. Numerals indicate the number of neurons recorded.

We next determined whether separate populations of axons were

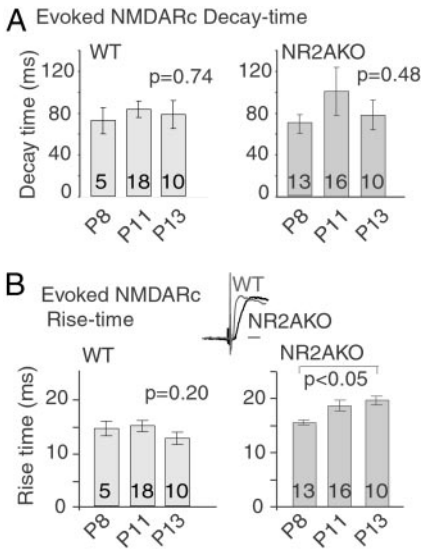

Fig. 2. NR2AKOs show no developmental changes in evoked NMDARc decay times but do show increases in rise time with age. (*A*) Decay times of evoked NMDARcs in WT and NR2AKO neurons were measured between P8 and P13. Evoked NMDARc decay times are indistinguishable between mutant and WT over this interval. (*B*) Rise times of evoked NMDARcs in WT mice were not significantly different with age. However, rise times of evoked NMDARcs in NR2AKO mice became significantly slower by P13 (two-tailed *t* test, $P < 0.05$). At P13, rise times in mutant neurons were also significantly slower than in the WT ($P < 0.05$). (Scale bar in *Inset* = 20 ms.)

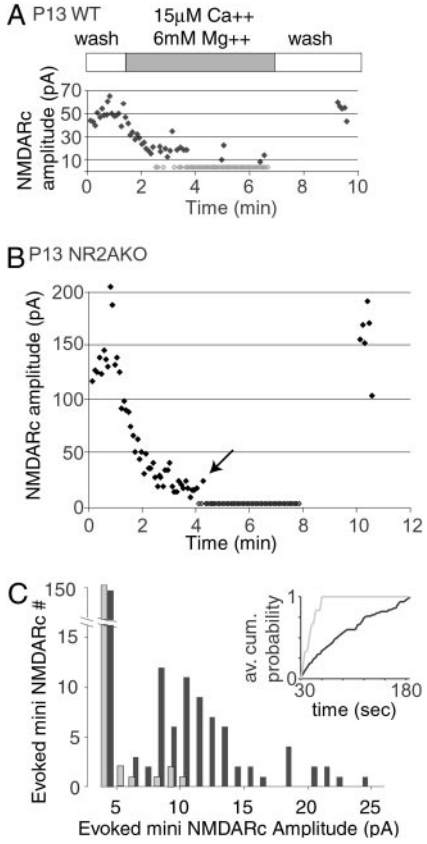

Fig. 3. On P13, ''evoked'' mini NMDARcs are present in WT mice but reduced in amplitude and number in NR2AKOs. Afferents were stimulated while the slice was perfused with low Ca^{2+}/high Mg^{2+} solution to reduce the probability of release. (*A*) Wash-in and wash-out of low Ca^{2+}/high Mg^{2+} in a WT neuron. Gray diamonds represent failures. (*B*) Wash in and out of low Ca^{2+}/high Mg^{2+} in a NR2AKO neuron. Note the absence of miniature events. (*C*) Amplitude/frequency histograms comparing evoked miniature NMDARcs in five WT and five NR2AKO neurons after completion of solution exchange (30 s after initial failure). WT cells (black bars) show two distinct amplitude populations around 9 pA and 18 pA. Fewer and smaller evoked miniature NMDARcs were recorded in NR2AKOs (gray bars). (*Inset*) The average cumulative probability of detecting evoked minis in five WT (black) and five knockout neurons (gray). The average frequency of evoked miniature events was 0.23 ± 0.04 in WT and 0.03 ± 0.02 in mutant mice.

responsible for mini and evoked NMDARcs. Evoked NMDARcs were detected in NR2AKO mice regardless of whether stimulation was applied to a neighboring sSC neuron through a lose patch electrode (data not shown) or to sSC afferents, suggesting that these NMDARs are close to presynpatic release sites. To determine whether synapses driven by the same inputs mediated both evoked and minis events, NMDARcs were elicited although low Ca^{2+}/high Mg^{2+} was perfused over the slice to reduce the probability of release. Evoked currents showed a smooth decrease in amplitude until "failures" (currents indiscernible from the 4-pA noise level at +40 mV) began to occur. Although WT neurons showed intermittent "evoked" mini NMDARcs, in NR2AKO neurons "evoked" minis occurred at one-tenth the frequency of WT and were significantly smaller (Fig. 3).

Spon/Mini NMDARcs Are Enriched for NR2A. Because NR2AKO mice lose spon/mini NMDARcs before any change is detected in the evoked current, we predicted that WT spon/mini NMDARcs may be enriched for NR2A and should have faster decay times compared with the evoked response. In P8 WT neurons, spontaneous and "evoked" mini NMDARcs had similar decay times (measured as 0.37 peak amplitude). However, by P10, decay kinetics of spon/mini NMDARcs in WT neurons were significantly faster than evoked responses (Fig. 4 *A* and *B*). In contrast, mini and evoked NMDARc decay times were indistinguishable in P10 NR2AKO neurons (Fig. 4 *A* and *C*). These results support the postulate that spon/mini currents in WT mice are mediated by NR2A-rich receptors, whereas evoked currents are mediated by both NR2A- and NR2B-containing receptors.

Ifenprodil, which preferentially antagonizes NR2B-containing NMDARs (20), was also used to test whether mini NMDARcs were preferentially mediated by NR2A-enriched receptors. Evoked NMDARcs were found to be significantly more sensitive to ifenprodil than either the evoked mini or spon/mini NMDARcs in the same cells (Fig. 4 *D* and *E*). The effect remained significant when data were corrected for small differences in evoked mini frequency before and after infenprodil (see *Methods*).

PSD-95 Selectively Associates with NR2A-Enriched Receptors. The expression of the NMDAR scaffolding molecule PSD-95, which is up-regulated during development, (21) was examined between P8 and P11. In visual neurons, NR2A and PSD-95 become highly enriched in dendrites within hours of eye opening (22), suggesting that normal increases in activity regulate the location of these proteins. We reasoned that, as in the truncated NR2A C terminus mutant (19), the inability of PSD-95 to scaffold NMDARs might account for the loss of miniature NMDARcs in the NR2AKO.

Western blots of synaptoneurosome protein isolated from the sSC of WT and knockout P8–P11 mice demonstrated that PSD-95 increases in this synaptically enriched fraction in both strains during the interval in which miniature NMDARcs gradually disappear in the NR2AKO (Fig. 5*A*). Coimmunoprecipitations of NMDAR subunits with PSD-95 and NR2B antibodies revealed significant reductions in the binding of both NR1 and NR2B subunits to PSD-95 in P11 NR2AKO sSC membrane

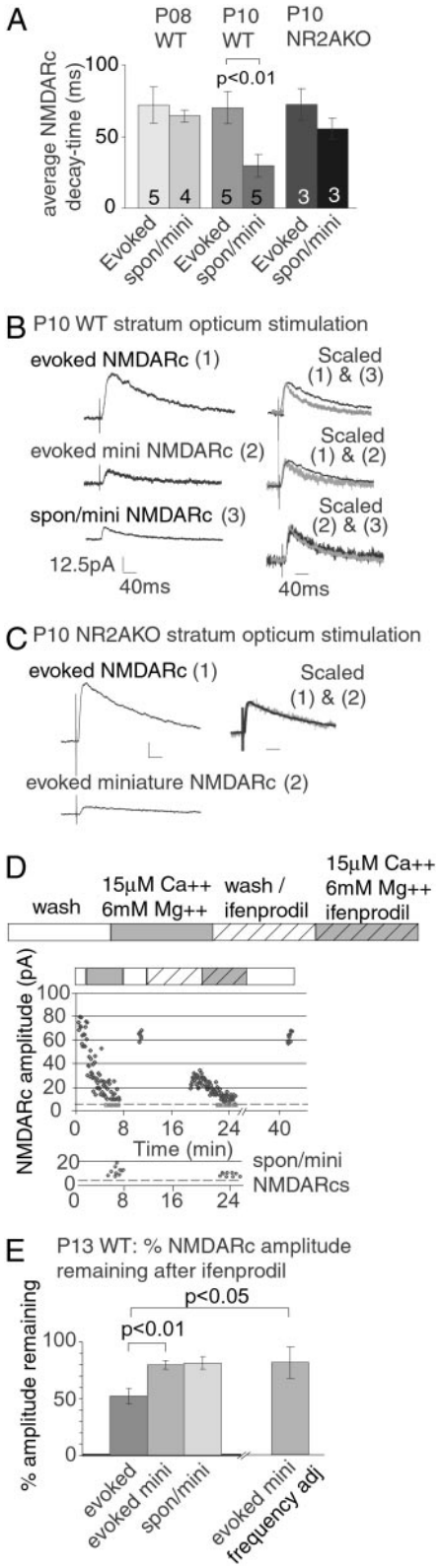

Fig. 4. Miniature NMDARcs in WT mice are enriched for NR2A. (*A*) By P10, the spon/mini NMDARc decay time is significantly reduced in WT but not NR2AKO mice. However, evoked NMDARc current decay time remains unchanged in both strains. (*B*) This effect can be seen within the same neuron. The decay kinetics of evoked, evoked mini, and spon/mini NMDARcs were compared in a P10 WT neuron. Traces depict average NMDARcs (11 evoked, 8 evoked miniature, and 21 spontaneous miniature NMDARcs). The evoked NMDARcs had slower decay times than either the spon/mini NMDARc (scaled 1&2) or the evoked miniature NMDARc (scaled 1&3). The kinetics of spon/mini and evoked miniature NMDARcs were indistinguishable (scaled 2&3). (*C*) Unlike WT mice, evoked and spon/mini NMDARcs had similar decay times in P10 NR2AKO neurons. Scale bars are the same as in *B*. (*D*) The NR2B specific antagonist ifenprodil was used to examine the subunit composition of evoked and miniature NMDARcs in P13 WT neurons. As in Fig. 3 *A* and *B*, evoked NMDARcs were recorded in normal and low calcium to isolate evoked and evoked miniature currents. This process was then repeated in the presence of 3 μM ifenprodil. Spon/mini NMDARcs (lower graph) were collected from the intervals between evoked minis. Dotted lines indicate thresholds of detectability (see Fig. 7). (*E*) Quantification of data from five P13 WT experiments showed that ifenprodil reduced the amplitude of the evoked NMDARc by 48 $\pm$ 6.8% SEM. In contrast, ifenprodil reduced the evoked miniature NMDARc by only 20 $\pm$ 3.9% SEM. Because evoked miniature NMDARcs are small and may be lost in noise after ifenprodil treatment, an additional calculation was made taking into consideration slight differences in evoked mini frequency (''evoked mini frequency adj''). Even with this conservative treatment, evoked NMDARcs were significantly more sensitive to ifenprodil than evoked miniature NMDARcs ($P < 0.05$).

fractions as compared with the same fractions in WT mice (Fig. 5 *B* and *C*). These results supported the idea that PSD-95 binding to NMDARs is significantly reduced in the NR2AKO (Fig. 5*B*) even though PSD-95 is up-regulated normally.

Between P10 and P11 in mice, the photoreceptor–bipolar–ganglion cell pathway begins to mediate the first visual responses (23, 24). Because this pathway uses glutamate as its primary transmitter (25, 26), photoreceptor-elicited activity in retinal ganglion cells was blocked by antagonizing glutamate receptors in the eye (see *Methods*). Animals were killed on P11, and synaptoneurosomes from the sSC contra- and ipsilateral to the blocked eyes were prepared separately. In WT mice, retinal block significantly ($P < 0.01$; Fig. 5*D*) decreased levels of PSD-95 and NR2A in synaptoneurosomes from the sSC contralateral (but not ipsilateral) to the blocked eye. Amplitudes of isolated spontaneous NMDARcs were measured in the sSC of P11 NR2AKO mice that were similarly treated or that had received sham Elvax. Retinal block had no effect on WT NMDARc amplitude, but significantly restored spon/mini NMDARcs in P11 NR2AKO mice (Fig. 5*E*). Thus the same disruption of normal retinal activity that slows PSD-95 and NR2A targeting to sSC synapses in WT animals, also delays the reduction in spon/mini NMDARcs amplitudes in the NR2AKO.

Discussion

NMDARs in the developing sSC are regulated by both subunit composition and an activity-dependent posttranslational mechanism (27). How the distribution of NMDARs in the postsynaptic membrane is regulated remains unclear. Immunoprecipitation and immunoelectron microscopy applied to developing hippocampus has revealed that the NMDAR scaffolding molecule SAP102 is prominent in the neonate, whereas PSD-95 levels rise later in the second postnatal week (21). These studies also showed that SAP102 is associated with NR2B rich receptors, whereas PSD-95 is associated with NR2A-rich receptors. Work in our own lab has revealed that eye opening causes a rapid, nearly 3-fold increase in PSD-95 protein and a simultaneous increase in NR2A association at the expense of NR2B in both sSC and visual cortex dendrites (22). Bidirectional changes in NMDAR subunit expression at visual synapses as a result of altered levels of activity have been described (12, 29). The present results as well as Yoshii *et al.* (22) implicate the PSD-95 in an activity dependent process that is associated with the addition of NR2A-rich NMDARs at synapses.

In the NR2AKO mouse, PSD-95 distributes to the membrane in the absence of NR2A, and is associated with the displacement of NR2B-enriched NMDARs from the center of the synapse to peri- and extrasynaptic sites as indicated by the loss of spon/minis, and

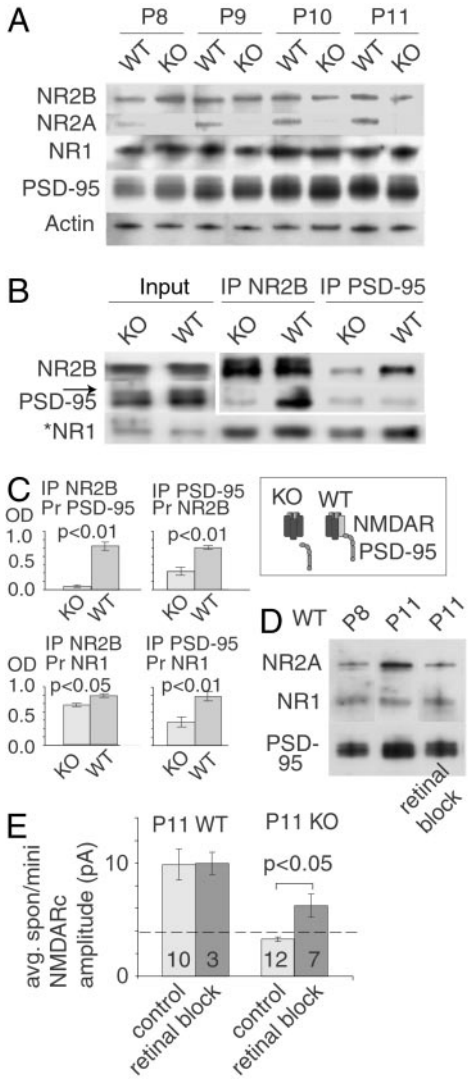

Fig. 5. PSD-95 increases in dendrites in WT and NR2AKO mice with visual activity, but preferentially binds to NMDARs containing the NR2A subunit. (*A*) Immunoblots of WT sSC synaptoneurosomes showed an up-regulation of PSD-95 and NR2A between P8 and P11 (mean P8 WT NR2A optical density = 0.73 ± 0.15 SEM; mean P11 WT NR2A optical density = 1.46 ± 0.15 SEM, mean P8 WT PSD-95 optical density = 0.60 ± 0.10 SEM, mean P11 WT PSD-95 optical density = 1.51 ± 0.10 SEM; ANOVA Tukey–Kramer post hoc, $P < 0.01$ comparing P8 to P11). NR1 and NR2B protein levels did not change over the same interval (ANOVA Tukey–Kramer post hoc, $P = 0.92$ and $P = 0.87$, respectively). Synaptoneurosomes from NR2AKO mice also showed PSD-95 increases (mean P8 knockout PSD-95 optical density = 0.72 ± 0.06 SEM; mean P11 knockout PSD-95 optical density = 1.3 ± 0.06 SEM; ANOVA Tukey–Kramer post hoc, $P < 0.01$). (*B*) Immunoprecipitations (IPs) with anti-PSD-95 antibody revealed a greater association among PSD-95, NR1, and NR2B in WT than in the NR2AKO mice. *, NR1 was probed in separate lanes, because the similar size of PSD-95 and NR1 confounded the quantitation (arrow in input lanes). Input lanes were diluted 5-fold. (*C*) Quantification of three separate protein isolations and three separate sets of IPs in WT and NR2AKO mice. (*Inset*) The suggested difference in NRMDAR/PSD-95 association between the knockout and WT. (*D*) Monocular infusion of AMPAR and NMDAR antagonists (P6-P11) into one eye of WT mice revealed that normal up-regulation of PSD-95 and NR2A did not occur in the contralateral sSC on P11 (ANOVA Tukey–Kramer post hoc, $P < 0.01$ comparing P11 to P11 retinal block). In contrast, the sSC tissue ipsilateral to the treated eye (second lane) showed the same increase in NR2A and PSD-95 expression as seen in *A*. (*E*) Amplitude decreases in NR2AKO spon/mini NMDARcs are reduced by retinal block of the contralateral eye. The treatment did not alter spon/mini amplitudes in WT, but restored the amplitude decrease seen in NR2AKO at P11. (Numerals represent the number of neurons studied.)

the prolonged rise time of evoked NMDARcs. Simultaneous with the developmental increase in PSD-95 and NR2A in synaptoneurosomes and membrane fractions, is a shift to NMDARc spon/minis with faster decay times consistent with the insertion of NR2A-rich receptors. Nevertheless, NR2B-rich receptors continue to dominate in evoked currents. These findings cannot be explained by altered transmitter release or cleft dimensions in the mutant, as AMPARcs and paired pulse responses appear normal. In addition, even single input stimulation in the mutant can be sufficient to evoke NMDARcs with no detectable minis, indicating that relatively small amounts of glutamate can diffuse to and bind these receptors, perhaps because of spillover from adjacent release sites or multiquantal release (30, 31). Recent work has stressed the importance of "extrasynaptic" NMDARs at hippocampal, retinal ganglion, and cerebellar granule cell synapses, and has upwardly revised estimates of the extent of glutamate diffusion from active sites (32–34). Our observations are consistent with electron mi-

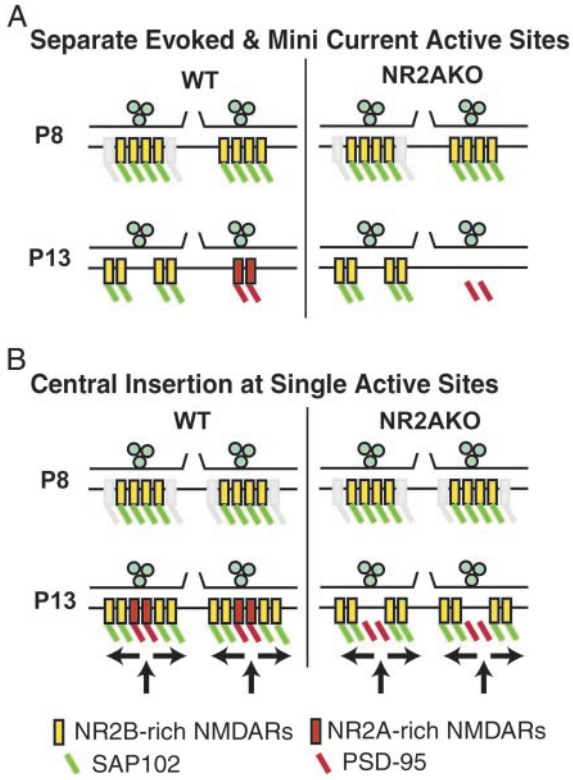

Fig. 6. Either of two models can account for the premature loss of miniature NMDARcs in the NR2AKO. (*A*) Separate synaptic active sites are responsible for evoked versus miniature NMDARcs. Synapses are shown in cross section with two adjacent active sites illustrated. P8 active sites have a similar composition in WT and NR2AKO mice. NR2B-enriched receptors are distributed across the postsynaptic membrane and are scaffolded, most likely by SAP102. By P13, two types of release sites are distinguishable. The first contains NR2B-enriched NMDARs, localized extrasynaptically, and mediating the prolonged decay time of evoked currents. A second population of release sites containing NR2A-enriched NMDARs, anchored by PSD-95, mediates miniature NMDARcs. The absence of NR2A in the mutant mouse leads to the loss of the second type of synapse. (*B*) Insertion of NR2A-enriched NMDARs at the center of all synapses also accounts for the data. On P8, active sites are indistinguishable between WT and NR2AKO mice. However, as a result of increasing photoreceptor-driven retinal activity, in P11 WT mice synapses with new NR2A-rich NMDARs bound to PSD-95 are inserted into the immediate subsynaptic membrane, where they mediate mini NMDARcs. Neonatal, NR2B-rich receptors are moved laterally to extrasynaptic sites. NR2AKO mice show a similar insertion of PSD-95 into the center of the synapse by P13. However, PSD-95 does not effectively bind NMDARs in the NR2AKO, and the activity-dependent insertion of PSD-95 produces an NMDAR-free "hole" in the center of the postsynaptic membrane.

croscopy data showing colocalization of both PSD-95 and NR2A at postsynaptic densities (35) and with reports that PSD-95 is highly concentrated at the postsynaptic density, whereas both SAP102 as well as PSD-95 are detectable at nonsynaptic membranes (36).

Two models representing the extreme versions of molecular trafficking that could account for our data are diagrammed in Fig. 6. The separate synapse hypothesis in Fig. 6*A* postulates that two types of NMDAR-containing synapses develop on the same postsynaptic cell; one mediates miniature events, and the other responds only when release is evoked. This model proposes that only one type of synapse undergoes a shift from NR2B- to NR2A-rich receptors as development proceeds. The remaining synapses independently lose central NMDARs although retaining extrasynaptic NR2B-rich NMDARs. The central insertion at single active site model shown in Fig. 6*B* hypothesizes that on P8, NR2B-enriched and SAP102-bound NMDARs are distributed at central and extrasynaptic positions. In WT mice, increases in activity target NR2A rich NMDARs bound to PSD-95 to synapses. The insertion of these complexes beneath release sites subsequently displaces neonatal NR2B-rich receptors. In both models, NR2A-dominated minis gradually replace NR2B-dominated mini NMDARcs, whereas evoked currents continue to activate peripheral NR2B-enriched NMDARs during the juvenile period. In the NR2AKO, both models predict that NR2B rich central receptors are lost if PSD-95 does not effectively scaffold NMDARs in the absence of NR2A.

Recent work in tissue culture suggesting that lateral movement of NMDARs into and out of synapses (37, 38) would favor the central insertion scheme. Indeed, the movement of nonanchored receptors away from the synapse has been proposed for the reduction of minis and prolonged rise times in NR2A C-terminal truncation mutants (19).

The present studies using intraocular glutamate antagonists to block photoreceptor to ganglion cell transmission were conducted before eye opening, during the interval when the first light-driven responses reach the central nervous system through closed eyelids. The observation that early increases in PSD-95 and NR2A in sSC dendrites can be blocked by reducing retinal output and that the same procedure reduces mini NMDARc loss in the NR2AKO suggest that increased localization of PSD-95 and NR2A at visual synapses can result from even relatively small changes in retinal activity. This finding is the strongest evidence that PSD-95 delivery to the synapses may be actively displacing earlier SAP102 anchored receptors. The mechanism of such a displacement is unknown. Because PSD-95 is palmitoylated, whereas SAP102 is not (39–41), perhaps PSD-95 is capable of associating with plasma membranes without binding to transmembrane receptors and may displace the SAP102 system as a result of this lipid association.

Regardless of which model or combination of the models proves correct, this and the accompanying paper (22) suggest that NR2A begins to replace NR2B-rich NMDARs in the sSC earlier in development than previously recognized, coinciding with the end of retinocollicular map refinement. These NR2A-rich NMDARcs are preferentially activated by single quantal events, and anchored by PSD-95. Although the functional significance of this is not yet clear, one possibility is that unique signal transduction cascades may be coupled to PSD-95 and SAP102. Alternatively, the kinetics Ca^{2+} flux mediated by NR2A-rich versus NR2B-rich receptors may have important implications for the type of signal generated (42). It will be important to determine whether subunit dependent changes in receptor binding affinities and kinetics, or synaptic versus peri- and extrasynaptic positions are differentially involved in the various developmental processes, activity-dependent gene activation (43), map refinement (14, 44), synapse elimination (45), receptive field development (46), and ocular dominance plasticity (28) in which NMDARs are thought to be involved.

We gratefully acknowledge valuable discussions with our colleagues H. Robert Horvitz, Ph.D., and Guosong Liu, Ph.D. This work was supported by National Institutes of Health Grant NS32290 (to M.C.-P.) and by National Institute of Mental Health Grant 5T32DA07290 and National Eye Institute Grant 5T32EY07115 (to M.T.).

1. Watanabe, M., Inoue, Y., Sakimura, K. & Mishina, M. (1992) *NeuroReport* **3,** 1138–1140.
2. Shi, J., Aamodt, S. M. & Constantine-Paton, M. (1997) *J. Neurosci.* **17,** 6264–6276.
3. Flint, A. C., Maisch, U. S., Weishaupt, J. H., Kriegstein, A. R. & Monyer, H. (1997) *J. Neurosci.* **17,** 2469–2476.
4. Hestrin, S. (1992) *Nature* **357,** 686–689.
5. Stocca, G. & Vicini, S. (1998) *J. Physiol.* **507,** 13–24.
6. Vicini, S., Wang, J. F., Li, J. H., Zhu, W. J., Wang, Y. H., Luo, J. H., Wolfe, B. B. & Grayson, D. R. (1998) *J. Neurophysiol.* **79,** 555–566.
7. Blakemore, C. & Van Sluyters, R. C. (1975) *J. Physiol.* **248,** 663–716.
8. Stryker, M. P. & Harris, W. A. (1986) *J. Neurosci.* **6,** 2117–2133.
9. Carmignoto, G. & Vicini, S. (1992) *Science* **258,** 1007–1011.
10. Nase, G., Weishaupt, J., Stern, P., Singer, W. & Monyer, H. (1999) *Eur. J. Neurosci.* **11,** 4320–4326.
11. Quinlan, E. M., Philpot, B. D., Huganir, R. L. & Bear, M. F. (1999) *Nat. Neurosci.* **2,** 352–357.
12. Philpot, B. D., Sekhar, A. K., Shouval, H. Z. & Bear, M. F. (2001) *Neuron* **29,** 157–169.
13. Ito, I., Sakimura, K., Mishina, M. & Sugiyama, H. (1996) *Neurosci. Lett.* **203,** 69–71.
14. Simon, D. K., Prusky, G. T., O'Leary, D. D. & Constantine-Paton, M. (1992) *Proc. Natl. Acad. Sci. USA* **89,** 10593–10597.
15. Scheetz, A. J., Nairn, A. C. & Constantine-Paton, M. (2000) *Nat. Neurosci.* **3,** 211–216.
16. Hollingsworth, E. B., McNeal, E. T., Burton, J. L., Williams, R. J., Daly, J. W. & Creveling, C. R. (1985) *J. Neurosci.* **5,** 2240–2253.
17. Johnson, M. W., Chotiner, J. K. & Watson, J. B. (1997) *J. Neurosci. Methods* **77,** 151–156.
18. Dunah, A. W., Luo, J., Wang, Y. H., Yasuda, R. P. & Wolfe, B. B. (1998) *Mol. Pharmacol.* **53,** 429–437.
19. Steigerwald, F., Schulz, T. W., Schenker, L. T., Kennedy, M. B., Seeburg, P. H. & Kohr, G. (2000) *J. Neurosci.* **20,** 4573–4581.
20. Williams, K. (2001) *Curr. Drug Targets* **2,** 285–298.
21. Sans, N., Petralia, R. S., Wang, Y. X., Blahos, J., II, Hell, J. W. & Wenthold, R. J. (2000) *J. Neurosci.* **20,** 1260–1271.
22. Yoshii, A., Sheng, M. H. & Constantine-Paton, M. (2003) *Proc. Natl. Acad. Sci. USA* **100,** 1334–1339.
23. Bansal, A., Singer, J. H., Hwang, B. J., Xu, W., Beaudet, A. & Feller, M. B. (2000) *J. Neurosci.* **20,** 7672–7681.
24. Molotchnikoff, S. & Itaya, S. K. (1993) *Brain Res. Dev. Brain Res.* **72,** 300–304.
25. Wong, W. T., Myhr, K. L., Miller, E. D. & Wong, R. O. (2000) *J. Neurosci.* **20,** 351–360.
26. Copenhagen, D. R. (1991) *Curr. Opin. Neurobiol.* **1,** 258–262.
27. Shi, J., Townsend, M. & Constantine-Paton, M. (2000) *Neuron* **28,** 103–114.
28. Bear, M. F., Kleinschmidt, A., Gu, Q. A. & Singer, W. (1990) *J. Neurosci.* **10,** 909–925.
29. Ramoa, A. S. & Prusky, G. (1997) *Brain Res. Dev. Brain Res.* **101,** 165–175.
30. Rusakov, D. A. & Kullmann, D. M. (1998) *J. Neurosci.* **18,** 3158–3170.
31. Silver, R. A., Cull-Candy, S. G. & Takahashi, T. (1996) *J. Physiol.* **494,** 231–250.
32. Arnth-Jensen, N., Jabaudon, D. & Scanziani, M. (2002) *Nat. Neurosci.* **5,** 325–331.
33. Chen, S. & Diamond, J. S. (2002) *J. Neurosci.* **22,** 2165–2173.
34. Clark, B. A. & Cull-Candy, S. G. (2002) *J. Neurosci.* **22,** 4428–4436.
35. Valtschanoff, J. G., Burette, A., Wenthold, R. J. & Weinberg, R. J. (1999) *J. Comp. Neurol.* **410,** 599–611.
36. Aoki, C., Miko, I., Oviedo, H., Mikeladze-Dvali, T., Alexandre, L., Sweeney, N. & Bredt, D. S. (2001) *Synapse* **40,** 239–257.
37. Barria, A. & Malinow, R. (2002) *Neuron* **35,** 345–353.
38. Tovar, K. R. & Westbrook, G. L. (2002) *Neuron* **34,** 255–264.
39. Chetkovich, D. M., Bunn, R. C., Kuo, S. H., Kawasaki, Y., Kohwi, M. & Bredt, D. S. (2002) *Neurosci. J.* **22,** 6415–6425.
40. El-Husseini, A. E., Topinka, J. R., Lehrer-Graiwer, J. E., Firestein, B. L., Craven, S. E., Aoki, C. & Bredt, D. S. (2000) *J. Biol. Chem.* **275,** 23904–23910.
41. El-Husseini, A. E., Craven, S. E., Chetkovich, D. M., Firestein, B. L., Schnell, E., Aoki, C. & Bredt, D. S. (2000) *J. Cell Biol.* **148,** 159–172.
42. Yang, S. N., Tang, Y. G. & Zucker, R. S. (1999) *J. Neurophysiol.* **81,** 781–787.
43. Hardingham, G. E., Fukunaga, Y. & Bading, H. (2002) *Nat. Neurosci.* **5,** 405–414.
44. Simon, D. K. & O'Leary, D. D. (1992) *J. Neurosci.* **12,** 1212–1232.
45. Colonnese, M. T. & Constantine-Paton, M. (2001) *J. Neurosci.* **21,** 1557–1568.
46. Tavazoie, S. F. & Reid, R. C. (2000) *Nat. Neurosci.* **3,** 608–616.